

# THE NUMERICAL INVESTIGATION OF A DUAL-MODE SCRAMJET COMBUSTOR

David Riggins  
University of Missouri-Rolla  
Rolla, Missouri

NAG 1-2167  
10-07

## ABSTRACT

A numerical investigation of a multiple-jet array dual-mode scramjet combustor has been performed utilizing a three-dimensional Navier-Stokes code with finite-rate chemistry. Results indicate substantial upstream interaction in the form of an oblique shock/expansion train upstream of the combustor, culminating in completely subsonic flow in the vicinity of fuel injectors. The flow returns to supersonic velocities in the downstream (diverging) portion of the combustor. Mixing and combustion are rapid in this flow and predicted combustion efficiency closely matches experimental data. However, comparisons of wall pressure between the simulation and the experiment show i) substantial underprediction of the upstream interaction distance and ii) moderate overprediction of peak pressure in the vicinity of the entrance of the combustor. This can be at least partially explained by examination of available experimental data; this data shows a very significant movement of the entering vitiated airflow to the sides of the combustor (around the injector array and the upstream interaction front as a whole). This important effect is currently being examined by an extension of the modeling to include the entire half-duct of the same combustor geometry.

## INTRODUCTION

The performance of a scramjet engine for flight Mach numbers above seven is characterized by bulk supersonic flow throughout the engine. Critical issues for such an engine include limited fuel-air mixing and reaction and irreversibilities caused by shocks, non-equilibrium reaction, and mass, momentum, and energy diffusion. Although there are complex interactions and trades between combustion and irreversibilities, and large contributions from fuel injection forces, combustion-generated heat release into the flow generally results in a net thrust force delivered to the hypersonic vehicle. However, such an engine is characterized by a relatively low ratio of heat release associated with combustion to entering enthalpy and by relatively high flow losses; thrust margins are relatively small. Many previous studies have focused on high Mach number flight in which bulk supersonic flow is maintained throughout the engine. Fluid dynamic separation and recirculation regions in such flow-fields are generally minimal; there is limited upstream interaction through boundary layers. Such flows are, for many purposes, adequately modeled using marching cycle solvers and more advanced multi-dimensional marching (parabolized) CFD codes. Where separation and recirculation do occur (as downstream of injector bases), modeling strategies have proven highly successful from an engineering analysis standpoint. Note that there are no throats in the pure scramjet engine, either physical or thermal in nature; the bulk flow remains supersonic from inflow to outflow.

The performance of a true ramjet engine in which combustion takes place entirely at subsonic velocities is also characterized in terms of flow losses and combustion. There are, however, physical throats located downstream of the combustor and upstream in the diffuser. Injectant forces generally

Approved for public release; distribution is unlimited.

\* This work was performed under NASA Grant NAG-1189 from the Hypersonic Vehicle Office at NASA Langley Research Center.

play a minor role in a ramjet. Combustion is not mixing-limited in such an engine. Due to the bulk subsonic region, information is readily transmitted from downstream to upstream. Fully elliptic Navier-Stokes codes suitable to low Mach number computations must, therefore, be used in order to correctly characterize ramjet engine performance. For example, a simple quasi-one-dimensional study of a ramjet flow readily demonstrates the coupling between downstream (combustor) heat-release, upstream normal shock placement (inlet position), and nozzle throat geometry. In the sense of upstream interaction, a ramjet flow-field is inherently more computationally demanding than a true scramjet flow-field. The performance of a ramjet degrades for Mach numbers above three due to several reasons. Thermal (material) limitations associated with stagnating the entering flow and the addition of combustion-generated heat into the flow demand that fuel flow rate be decreased in order to maintain acceptable temperatures at the end of the combustor. With a maximum specified (allowed) temperature, even an ideal ramjet has a maximum Mach number at which fuel flow rate and hence thrust is zero. Secondly, increasing irreversibilities and disassociation associated with the inlet diffusion process begin to overwhelm any possible thrust benefits from the achievement of subsonic combustion. These performance issues limit a ramjet engine to flight Mach numbers of 4 to 5.

Mid-speed scramjet air-breathing propulsion systems have an inevitable transition region from Mach 4 to Mach 7 in which a ram-only design or a scram-only design view of the internal flowfield is insufficient. Operation of an engine in this critical transition regime is generally termed as dual-mode, implying mixed characteristics of both subsonic and supersonic flow or active transitioning between subsonic and supersonic combustion within the engine. The flow in this regime is characterized by combustion-related upstream interaction (flow effects due to downstream combustion which occur upstream of the combustor entrance and the fuel injectors); this generally takes the form of an oblique or normal shock train within an upstream duct called an isolator. The function of an isolator in the dual-mode engine is to effectively 'isolate' the inlet flow-field from any combustor-generated upstream interaction in order to prevent inlet unstart and operability problems. The mechanisms which generate the upstream oblique waves are upstream-propagating boundary-layer growth and large recirculation regions. These originate due to adverse pressure gradients developing in the combustor coupled with thermal choking of the bulk flow (see Figure 1). This thermal throat occurs due to the pressure rise in the isolator through the oblique shocks (corresponding to a lower combustor Mach number) and the heat release in the combustor. The flow in such a case is complex, transitioning, and is not well understood at this time; yet dual-mode operation is critical for the achievement of air-breathing flight above Mach 5. Fully elliptical computational techniques and solvers are required in order to adequately model such flows. This investigation centers on the numerical simulation of a dual-mode combustor flow-field in which significant upstream interaction is shown in experimental data. The specific goals of the present study are: i) to provide understanding of dual-mode flow physics by simulating a dual-mode flow-field using a full Navier-Stokes code and ii) (ultimately) to provide analysis of convergence acceleration techniques for such problems. The experimental case analyzed here is a recently available dual-mode combustor test performed at the National Research Laboratory in Japan.

Characterization of the complex flow-field in dual-mode scramjets (first introduced by Curran and Stall [1] in 1963) has been the subject of a number of previous investigations; Billig, et al. and Waltrup, et al., [2], [3], [4], [5] first provided analysis of experiments and analytical tools allowing

## DESCRIPTION OF EXPERIMENT

The experiment modeled in this numerical investigation was performed at the National Aerospace Laboratory in Japan and is extensively documented in a number of references, [9], [10]. A brief summary of the experiment (as reported in these references) is as follows: the experimental apparatus consists of a vitiated air heater and a Mach 2.5 facility nozzle with its expansion direction matched to the combustor width (rather than to the combustor height). Figure 2 shows a sketch of the experimental set-up for the nozzle, isolator/combustor and downstream combustor. The isolator extends .22 m upstream of the combustor entrance, which is located at  $x = 0$  and coincides with small backward-facing steps. The upstream isolator is rectangular in cross-section (.1473 meters wide by .032 meters high). The steps at the combustor entrance are .0032 meters high; the combustor is thus .0384 meters high and .1473 meters wide and is constant in cross-section until  $x = .096$  when top and bottom walls expand at 1.7 degrees while maintaining constant width. The nominal length for the combustor for this investigation is taken as .4 meters as back-pressure effects were observed beyond that station in the experiment. Fuel injection occurs at  $x = .013$ m (just downstream of the back-facing steps at the entrance to the combustor). There are five equally spaced fuel injector orifices on the bottom wall with spacing between injectors set at .032 meters. There are four interdigitated injector orifices on the top wall with the same spacing between injectors. All hydrogen fuel injection is sonic and normal to the combustor walls. The diameters of the two side injector orifices on the bottom (five) row were reduced such that one-half of the mass flow rate of hydrogen from each was injected (relative to the main injectors); this was apparently done in order to equally fuel top and bottom halves of the combustor.

A large amount of data was taken in these experiments for a number of duct lengths, array geometries, fuel equivalence ratios, etc. The test run of interest in this study was with geometry as indicated above, total fuel equivalence ratio of 1.0, total temperature of vitiated airflow of 2000K, total pressure of vitiated airflow of 1 MPa and composition of vitiated airflow nominally at mass fractions for oxygen, water, and nitrogen respectively of .24, .17, and .59. The conditions gleaned from the experimental references for the test run analyzed in this investigation are given in Table 1. This case was chosen for numerical simulation due to the large upstream interaction (dual-mode characteristics) clearly shown in the available experimental pressure data.

## COMPUTATIONAL METHOD

A computational fluid dynamics code derived from the original SPARK family of CFD codes (developed in the late 1980's at NASA LaRC by Drummond [15]) has been used for all computations in this investigation. This code utilizes an explicit time-marching full Navier-Stokes solver and contains a general finite-rate kinetics (chemistry) package. It has been extensively validated for higher speed internal scramjet combustor problems in previous investigations. The dual-mode combustor flow-field must be simulated utilizing the full Navier-Stokes capability due to the extensive upstream interaction and separated zones. The code is not well-suited in terms of efficiency for largely subsonic problems and requires small time steps and hence many iterations for such flows. However, due to the mixed-mode fluid dynamics present in mid-speed scramjet combustor flow-fields, this code was determined to be suitable for preliminary analysis and in particular for the ongoing investigation of candidate convergence acceleration techniques for dual-mode problems.

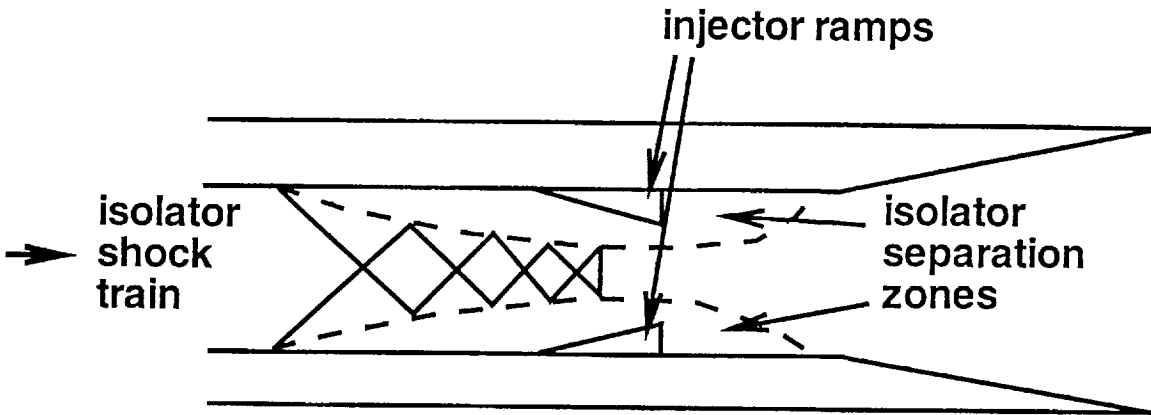


Figure 1 Schematic of dual-mode flow-field in scramjet combustor

the prediction of upstream interaction, required isolator length required, etc., for mid-speed scramjet combustor configurations. A well-known correlation for upstream interaction distance was formulated; dependence is in terms of heat release (downstream pressure rise) and entering momentum characteristics of the boundary layer before isolator separation. More recently, Anderson [6] at NASA Langley Research Center studied mid-speed scramjet combustor performance and determined that expansion steps upstream of the combustor yielded some degree of isolation from pressure wave interaction the upstream flow. Other early work performed at NASA Langley Research Center involving flows analyzed experimentally which had some degree of dual-mode characteristics include that of McClinton [7] and Eggers, et al. [8]. Experimental studies in Japan have been performed by Komuro, et al. [9], [10] and further reported on by Chinzei, et al. [11]. The experimental configuration detailed in these last papers and reports are the focus of the present numerical investigation. Recent computational studies of the same configuration are presented in [12] and [13]. There is a thorough and extended treatment of dual-mode flow-fields by Heiser and Pratt [14].

The second section of this paper provides a brief review of the experimental configuration. The third section is a review of the computational method and approach used in this investigation. Results of the numerical study are presented and discussed in the following section with comparisons to experimental data and an analysis of the discrepancies between the experimental data and the numerically predicted flow-field. The last section provides a summary of the investigation, ongoing work and recommendations regarding the numerical simulation of dual-mode flow-fields.



Table 1 Conditions for National Aerospace Lab (Japan) Dual-Mode Scramjet Experiment

INFLOW:

(Nominal)

Inflow from conventional Mach 2.5 Laval nozzle

Mach = 2.5

initiated inflow (see below)

static pressure = 55,222 N/m<sup>2</sup>

static temperature = 1009K

density = .17642 kg/m<sup>3</sup>

gas constant (R) = 316 J/kgK

gamma (ratio of specific heats) = 1.3085

velocity = 1630 m/s

incoming boundary layer thickness ~ .01m

mass fraction O<sub>2</sub> = .24335

mass fraction H<sub>2</sub>O = .1710

mass fraction N<sub>2</sub> = .5835

mass flow rate (total) = 1.355 kg/s

INJECTION:

Hydrogen

Mach = 1.0 (normal)

static pressure = 355,000 N/m<sup>2</sup>

static temperature = 233.3K

velocity (normal) = 1161 m/s

discharge coefficient = .85 (approx)

diameter of throat (orifice) = .004m/.0028m

9 injectors: 5 bottom/4 top (interdigitated)

gap between injectors = .032m

mass flow rate of fuel (total) = .0414 kg/s

COMPUTATIONAL DOMAIN:

.016m (width) X .0192m (height) at plane of injectors

symmetry/anti-symmetry/symmetry/no-slip

adiabatic

inflow mass flow rate = .074 kg/s

fuel injection mass flow rate = .00259 kg/sec (½ centerline injector)

Two modifications have been made to this code in order to perform dual-mode combustor analysis. The first modification enables internal domain rollover within the integrator which in turn allows the rapid development of the initial flow-field for large-scale elliptic problems. The second feature is the recent addition of the  $k-\omega$  two equation turbulence model [16] to the code along with the Mentor modification to that model [17]. This turbulence model has been shown to be robust for flows with both separation and highly adverse pressure gradients (both critical and dominating phenomena for dual-mode problems). The turbulence model is simply implemented in a de-coupled fashion within the explicit time-marching structure of the existing code; due to the small explicit time steps which are already mandated by the code, there has been no convergence problems or issues observed with this model. Validation of this model as implemented into the code has been on simple flat plates with favorable comparison to published results. This model is believed to represent the application-level state-of-the-art turbulence strategy and is present in most mainstream (widely used) CFD codes. Turbulent mass diffusion is modeled in this study assuming a constant turbulent Schmidt number of .5. Turbulent diffusion of heat is similarly modeled using a turbulent Lewis number of 1.0.

A seven reaction-seven species finite-rate chemical kinetics model [15] has been used in this work. Also, a related investigation using a complete reaction-based method (fast chemistry) with a reaction efficiency of .8 has been completed; little significant difference in results between the techniques were observed.

The domain modeled in this investigation includes the separate solution of a Mach 2.5 facility nozzle flow-field using a  $61 \times 61 \times 26$  grid. This solution is obtained over one-quarter of the full nozzle from nozzle throat to nozzle exit plane, i.e., from nozzle centerline to nozzle expanding wall and duct centerline to lower wall. The 3-D simulation of this flow-field is necessary due to the fact that the nozzle expands to the width (rather than the height) of the combustor duct. Although the nozzle nominally provides Mach 2.5 flow to the isolator/combustor, computations have resulted in a flow-field strip being provided to the centerline injector array which has a maximum Mach of about 2.4. This nozzle solution represents a preliminary analysis (i.e., an improvement over the assumption of uniform inflow or an inflow generated by modeling an upstream duct) and is expected to be refined in future work. The top and bottom boundary layers existing at the nozzle exit are about 1 centimeter in thickness (at the entrance to the isolator).

The main isolator-combustor solution domain is modeled from bottom jet centerline to opposing jet centerline (on the top wall), from bottom to top wall of the duct, and from the beginning of the isolator (at  $x = -.22\text{m}$ ) to the end of the nominal combustor duct (at  $x = .4\text{m}$ ). The solution is obtained utilizing a total grid of 301 (axial) by 41 (transverse) by 51 (vertical), although the use of anti-symmetry conditions ultimately reduced grid requirements by a factor of two (see Figure 2). Symmetry conditions were taken on both jet centerlines (side boundaries), anti-symmetry on top duct centerline, and no-slip was applied on the (bottom) combustor/isolator wall. Linear extrapolation was used on the outflow while, as noted above, inflow was provided by a preliminary simulation of the facility nozzle flow-field. Adiabatic walls were assumed everywhere based on information supplied in [13]. Table 1 provides the nominal inflow and injection conditions used in this study.

The hydrogen fuel is injected normal to the flow at sonic velocity. Note that, as mentioned in the previous section, the two side injectors on the bottom (five orifice) array each had one-half of the fuel mass-flow rate of the other injectors. This effect is not accounted for in the numerical study due to the sub-domain modeled and the symmetry assumed.

## RESULTS

This section describes the computational results obtained for the dual-mode scramjet combustor configuration discussed in previous sections.

Figure 3 presents pressure contours on a detail of the longitudinal plane through the bottom jet centerline. The primary feature is the substantial development of upstream interaction. A strong upstream shock/expansion train is established beginning at approximately .11m upstream of the step (.123m upstream of the injectors). Contour levels have been selected in Figure 3 in order to highlight the upstream pressure contours rather than the injection flow-field. Figure 4 shows velocity vectors in the same plane; these vectors provide clarification for the flow patterns observed in Figure 3. The initial oblique shocks from both top and bottom wall are caused due to large recirculation zones on top and bottom walls. These recirculation regions extend upstream from the backward-facing steps to the initialization of the oblique shocks in the isolator. They are characterized by patterns of increasing and decreasing height in the axial direction, yielding a distinct diamond-like appearance which can be observed in the velocity vector field (Figure 4). The initial oblique shocks reflect strongly at the centerline of the duct; the core flow (which is still supersonic) then passes through a short expansion fan due to the first constriction of the recirculation zones. The core flow then encounters a second oblique shock pattern as the recirculation zone again increases in height. This second oblique shock structure strongly reflects at duct centerline (at about  $x = -.05\text{m}$ ). This is followed by yet another (weak) expansion (again due to the undulating character of the recirculation zone) and finally the flow passes through a weak shock/Mach wave at  $x = -.03$  meters. The flow downstream of  $x = -.03$  is, in fact, entirely subsonic (until well downstream of the injection region). Figure 5 shows Mach number contours in the region of the upstream interaction/injectors for the same longitudinal plane. The shock/expansion pattern in the supersonic core followed by eventual deceleration to entirely subsonic flow is clearly visible in terms of Mach number. Note that although the jet is highly pressurized with respect to the entering free-stream from the facility nozzle, the overall pressure in the vicinity of the step and injector region is approximately the same as the injector static pressure. This is due to the pressurization caused by the fuel/air reaction and the choking of the flow. Because of this rough equality in pressure between jet and combustor flow, there is little expansion of the jet evident in Figures 3-5. The jet exhausts at essentially matched pressure into a large, uniform, high-pressure, and entirely subsonic region. Although corresponding figures of pressure contours, velocity vectors, and Mach contours for longitudinal planes between jet centerlines are not shown here, the flow-field across the width of the domain is very uniform in terms of degree/length of upstream interaction, character of separation zones, etc. This tendency to two-dimensionality of the upstream zone will be significant later when the results of the simulation are compared in terms of wall pressure with experimental wall pressure traces. The bulk downstream flow becomes supersonic again at about  $x = .14\text{m}$  (downstream of the

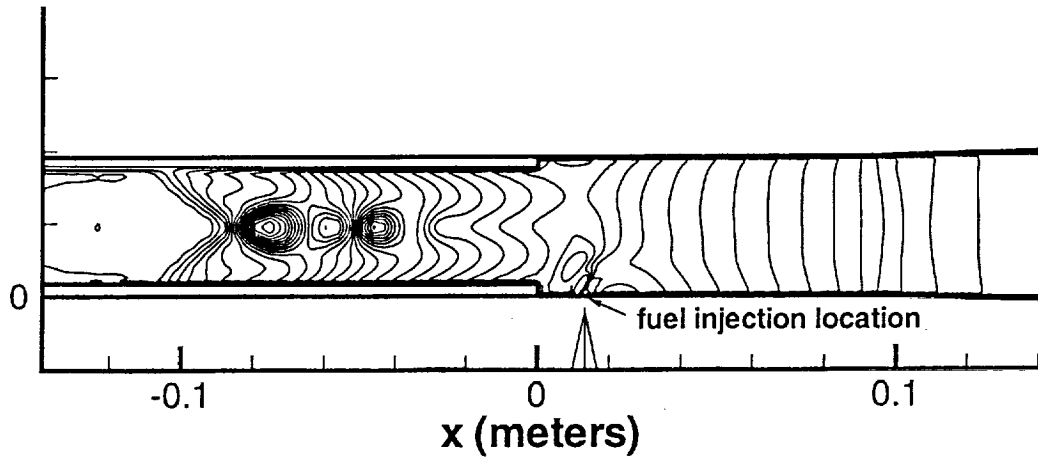


Figure 3 Pressure contours on longitudinal jet-centerline plane (detail) showing upstream interaction and fuel injection

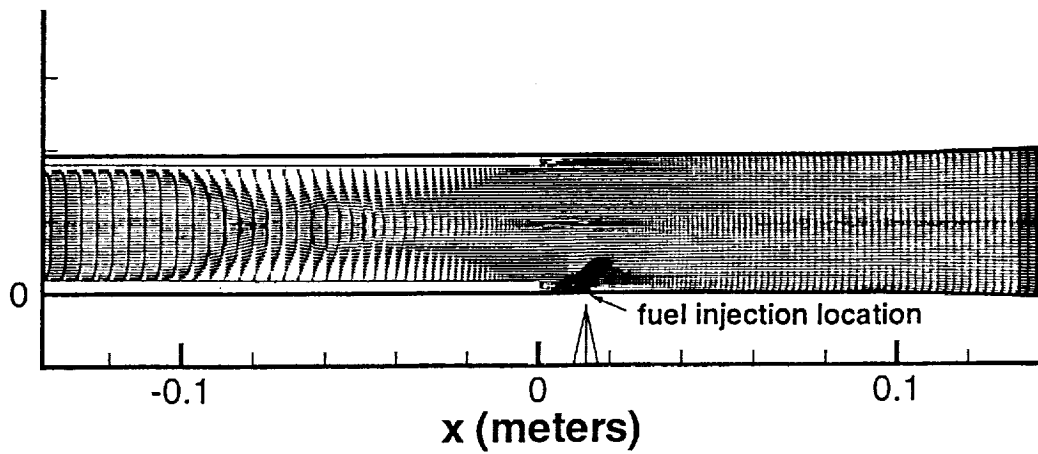


Figure 4 Velocity vectors on longitudinal jet-centerline plane (detail)

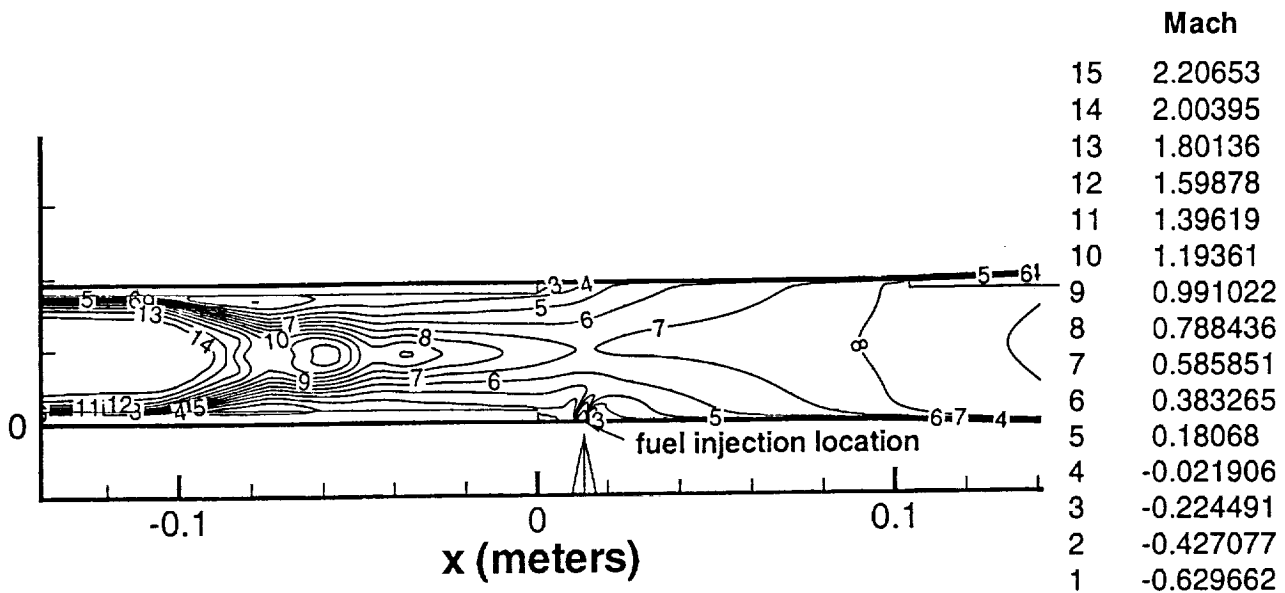


Figure 5 Mach number contours on longitudinal jet-centerline plane (detail) showing upstream interaction and fuel injection

backward-facing steps). This corresponds to an axial location located slightly into the diverging part of the combustor. The observed characteristic of the flow in moving from supersonic upstream to completely subsonic (in the injection region) and back to supersonic (in the downstream combustor) follows the analysis of the experimental data presented in [9].

Figure 6 illustrates water mass fraction contours on the same jet centerline plane, again in the vicinity of the injection and isolator. Significantly, no entrainment of fuel (or reacted water) upstream of the steps is observed; i.e., no reaction upstream of the injectors takes place even though there is massive upstream interaction. This is due to the truncation of the upstream separated zones at the steps; fuel does not negotiate upstream over the backward-facing steps and into these regions. The upstream interaction is formed and configured solely by the pressure rise associated with the downstream exothermic reaction. This pressure rise is communicated upstream through the bulk subsonic flow around the injectors and the upstream steps.

Figure 7 is a contour plot of the viscosity on the same centerline longitudinal plane and illustrates the presence of the boundary layers, jet-freestream shearing, and shock interactions. The viscosity in the numerically-generated flow-field is based on the  $k-\omega$  (Menter modification) turbulence model which in general displays reasonable behavior for flows with large pressure gradients and separated flow-fields.

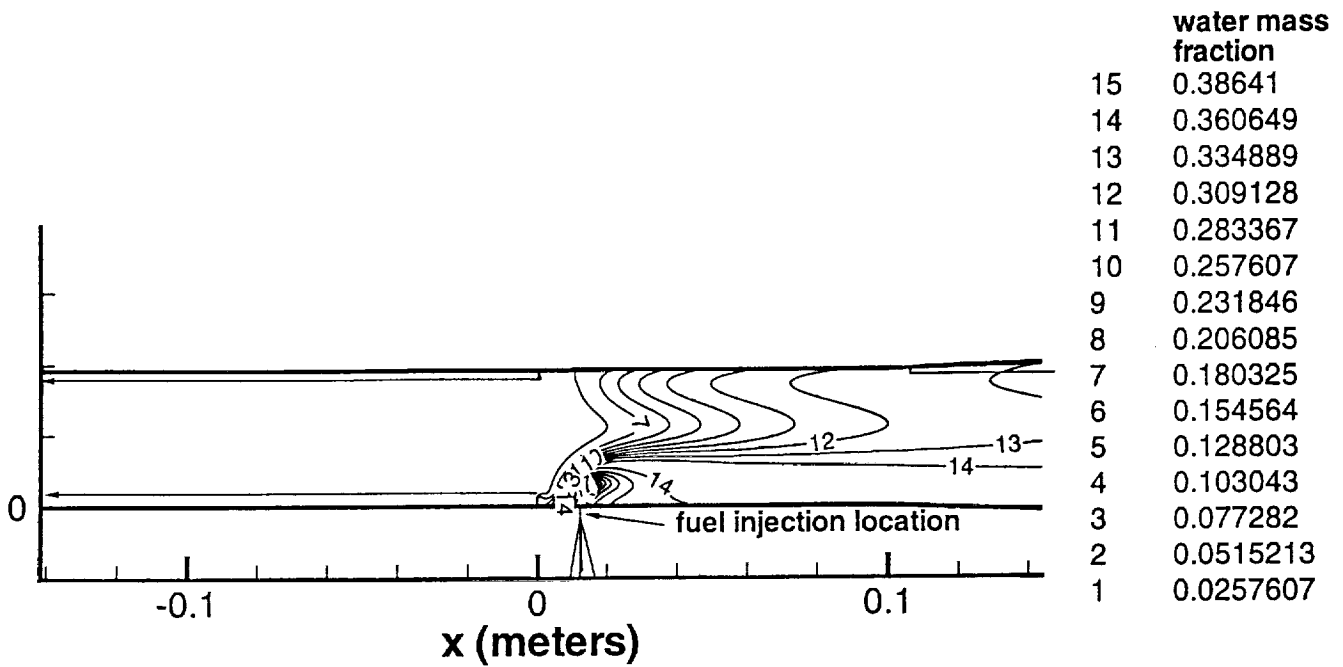


Figure 6 Water mass fraction contours on longitudinal jet-centerline plane (detail) in vicinity of combustor entrance

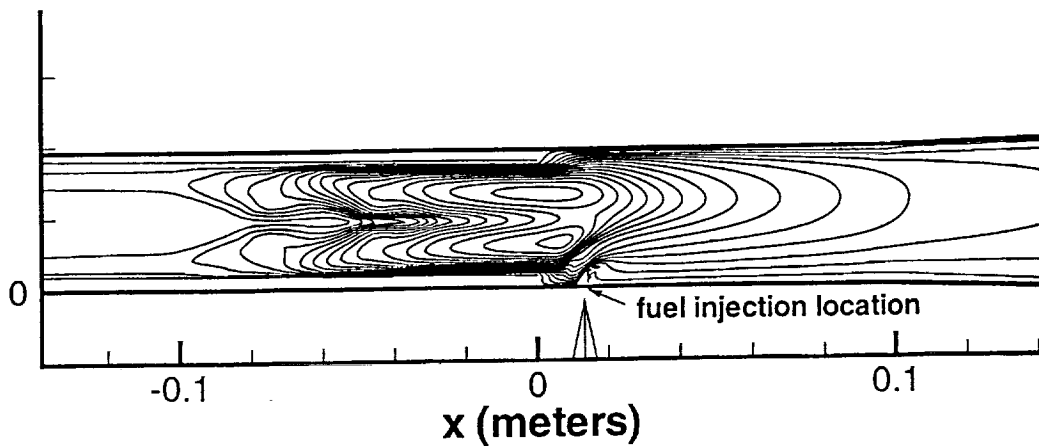


Figure 7 Viscosity contours on longitudinal jet-centerline plane (detail) in vicinity of combustor entrance

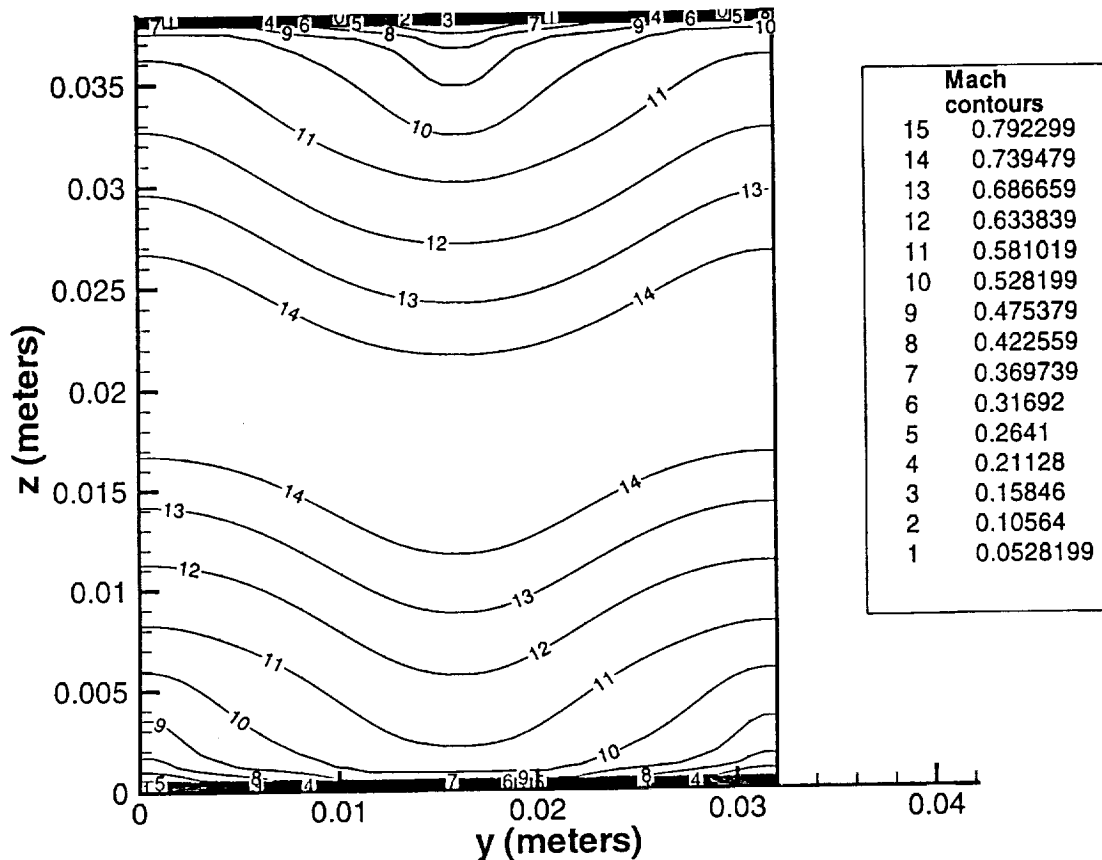


Figure 10 Mach number contours on cross-flow plane ( $x = .043\text{m}$ ) just downstream of injectors

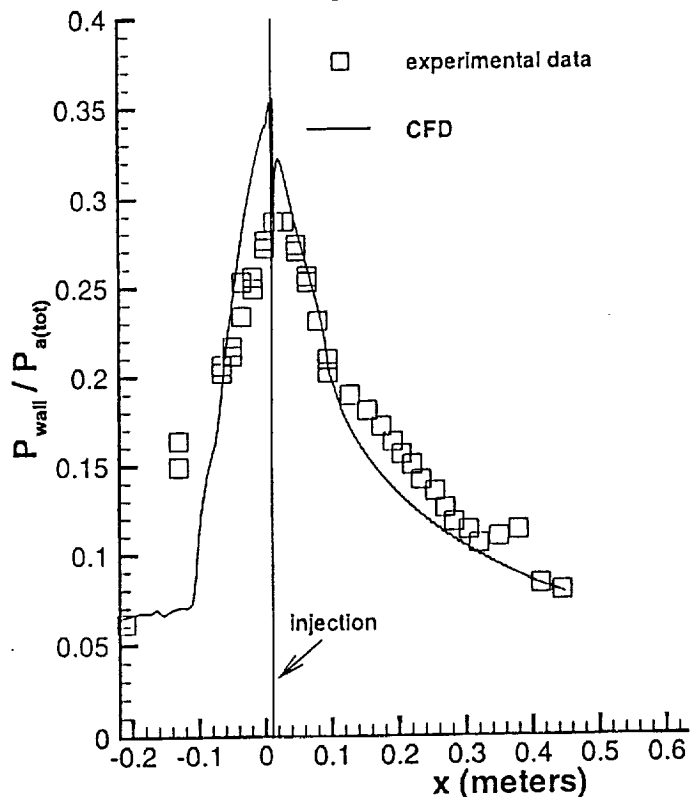


Figure 11 Experimental and CFD-predicted wall pressure distribution

Figure 8 is a crossflow contour plot for water mass fraction (located at  $x = .043\text{m}$ ). This contour plot extends from jet to adjacent jet centerline. Note that the inflow is vitiated with approximately 17% water by mass. Figure 8 shows the ring-like zones of maximum water corresponding to exothermic reaction around each jet core. There is little evidence of any action of spillage-induced vortices which figure so prominently in high-speed combustor flows. However, it should be noted that mixing and combustion are nevertheless quite rapid in this flow. This is believed due to the subsonic nature of the flow in the vicinity of the injectors.

Mixing and combustion efficiency axial distributions as predicted by the simulation are shown in Figure 9. Combustion efficiency is based on actual water production due to reaction; mixing efficiency represents the maximum potential combustion efficiency based on fuel-oxygen mixed. Note the steep rise in both parameters; the difference in the two parameters across the range is due to product species other than water (i.e., OH, H, O). Also shown on the plot are experimentally derived combustion efficiencies. The CFD slightly overpredicts these efficiencies but overall agreement is very good.

The completely subsonic nature of the flow in the vicinity of the injectors is further seen by examining Mach number contours on a crossflow plane (again at  $x = .043\text{m}$ ) just downstream of the fuel injectors (Figure 10). There is only slight evidence of jet structure in either Mach number or velocity vectors at this near-field cross-flow plane. Although entirely subsonic at this station, the flow rapidly resumes supersonic character further downstream. The tendency of the subsonic flow to return to supersonic in the downstream section of the combustor demonstrates the critical importance of multi-dimensional CFD for the dual-mode combustor problem. As shown here, such a flow is dominated by fluid-thermal throats and complex upstream oblique shock/expansion patterns. Although this particular flow-field is characterized by embedded subsonic flow (no supersonic core at the location of the injector array, as predicted by CFD in this investigation and verified by experimental results in [9]), some dual-mode flow-fields, although characterized by very large subsonic and recirculatory flow regions, have a persisting supersonic core. It is, in fact, this variability between fully subsonic, fully supersonic, or mixed-mode fluid dynamics, which makes the dual-mode problem so challenging.

Figure 11 provides the axial distribution of experimental wall pressure versus numerical results for this problem. There are two significant discrepancies between the CFD and the experimental results. First, the extent of upstream interaction is significantly underpredicted. The experimental wall pressure trace indicates that the upstream interaction (pressure rise) begins about .15 to .16m upstream of the steps. The numerical results show upstream interaction (pressure rise) beginning at about .11m upstream of the steps, representing a 30% underprediction in interaction distance. Secondly, there is some overprediction of maximum pressure (approximately 15%) at and near the step itself. The downstream pressure matches the experimental results fairly well - note that small spikes (jags) in the experimental pressure trace seem to correspond closely with nozzle block boundaries indicating possible small mis-alignments in the experiment - this, however, has not been verified. Overall, the trend and magnitude of the pressure characteristics of this flow-field are well-represented, with the two important exceptions noted above. Note that the experimental upstream

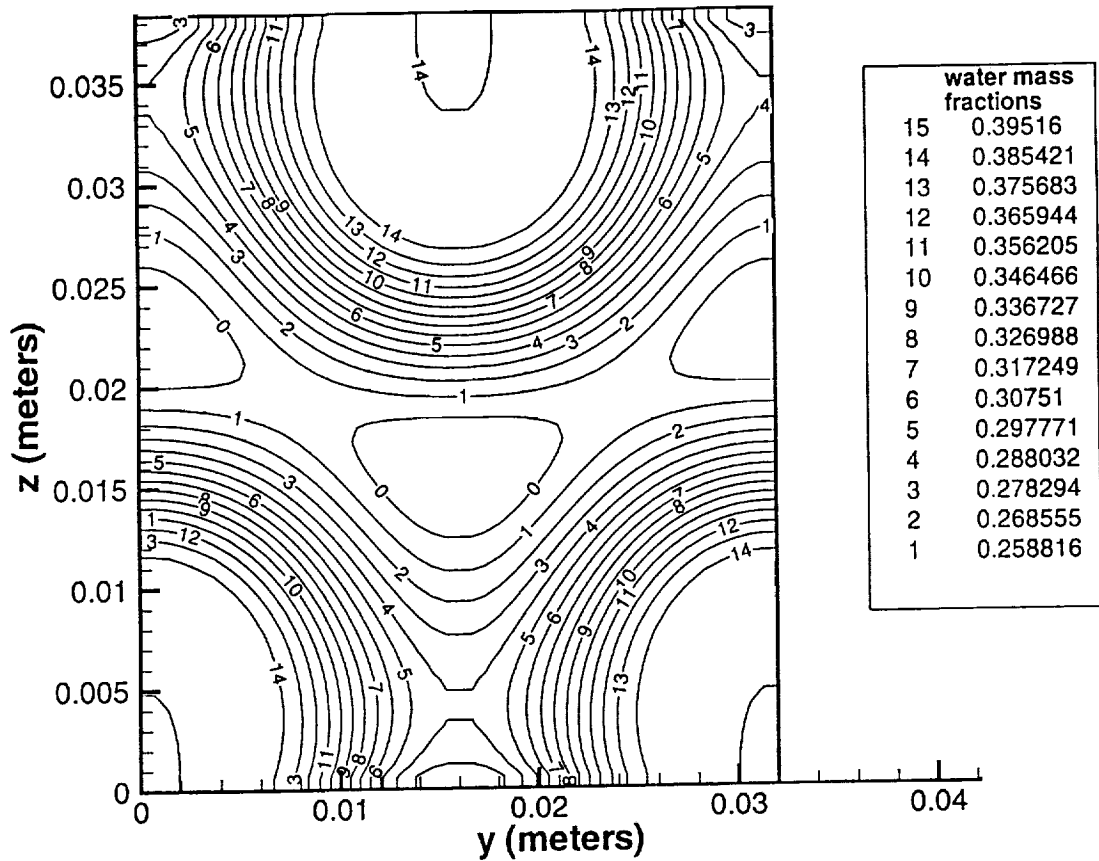


Figure 8 Water mass fraction contours on cross-flow plane ( $x = .043\text{m}$ ) just downstream of injectors

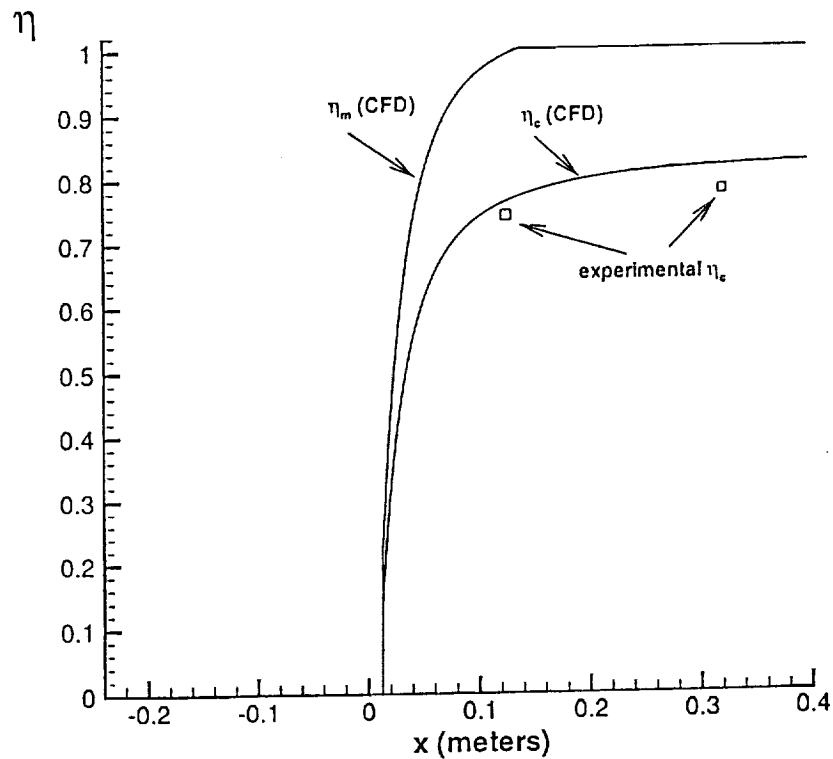


Figure 9 Mixing and combustion efficiency axial distributions

interaction distance is itself significantly lower than that indicated by the correlation of Ref. [4]. However, as noted in [11], the correlation is based on a no-step cylindrical combustor step; the steps significantly impact details of the upstream interaction zone. Furthermore, there is a large dependency on total temperature which is not accounted for in the correlation.

It is at first tempting to attribute the underprediction of the upstream interaction zone within the CFD results (as well as the overprediction of peak pressure) to turbulence modeling inadequacies in the CFD solver. There is, in fact, a historical trend in underprediction by CFD of the upstream interaction length for dual-mode problems. The impact of turbulence modeling in correctly representing such flows is very well known. In this case, however, careful examination of the available experimental data has led to an alternate conclusion. For this flow, there is strong evidence that there is a significant amount of three-dimensionality to the flow-field which enters and traverses the combustor. Specifically, examination of downstream (experimental) fuel contours on crossflow planes show a clear movement of entering air to either side of the bulk array of injectors, such that the true bulk fuel-equivalence ratio on the combustor centerline is close to 1.5 (rather than the nominal 1.0) and falls to very low values near the sides of the test section. Furthermore, the flow provided to the isolator/combustor comes from a facility nozzle which is oriented with its expansion direction corresponding to the width (rather than the height) of the isolator/combustor (see Figure 2). Contours of experimental pitot pressure exhibit significantly lower energy flow at the nozzle exit along the duct centerline - which is exactly where the experimental pressure taps are located. These two related effects; nozzle flow characteristics and the bulk movement of the airstream around the entire injector array (hence lowering the mass and energy of the vitiated inflow into the centerline jets) would tend to i) increase the experimental upstream interaction distance (lower energy inflow at centerline) and ii) decrease the observed experimental pressure around the injector (fuel equivalence ratio significantly above 1.0). Both effects are clearly demonstrated in a comparison between the CFD results and the experimental results in Figure 11. The discrepancies between CFD and experiment can thus be explained tentatively by this observation.

The three-dimensionality in the experiment undermines the validity of the assumption of jet-to-jet symmetry for the flow-field entering the combustor for this case. In fact, the use of jet-to-jet symmetry boundary conditions in CFD for such problems must be handled with caution and may have to be discarded. For this case, specifically, one-half of the entire cross-section of the duct must be modeled in order to account for the phenomena discussed above. This pronounced effect of the airstream 'seeing' the separated zones far upstream of the injector array as a bulk obstacle and subsequent large-scale turning of the core flow to the sides of the entire test section may be a common and critical issue in attempting to numerically model such dual-mode problems. It is expected that high aspect ratio multi-injector array combustors will not be as strongly impacted by this phenomena as lower aspect ratio combustors such as that analyzed in this investigation. Although modeling the entire half-width of the combustor/isolator is difficult from the standpoint of computational resources, it is possible and is currently being done as a continuation of this investigation.

## SUMMARY

A dual-mode scramjet combustor configuration which has experimental data indicating substantial upstream interaction has been modeled numerically. Numerical results show the development of substantial upstream interaction consisting of an oblique shock/expansion train. This shock/expansion system is generated by large recirculation zones on both top and bottom isolator walls; separated zones extend from well into the isolator to small backward facing steps at the entrance to the combustor. The recirculation zones have a pattern of increasing and decreasing heights which generates progressive oblique shocks and weak expansions. The flow is diffused by this system and becomes entirely subsonic well before the entrance to the combustor and the fuel injection region. In the combustor, fuel is injected from top and bottom linear arrays of normal flush-wall fuel injectors. The pressurization of the flow-field due to exothermic reaction and diffusion results in nearly matched pressure injection. There is no entrainment of the fuel or reacted water upstream of the combustor entrance (i.e., upstream over the edges of the backward facing steps) observed in the numerical simulation. The massive upstream interaction occurs due to downstream pressurization of the flow and is not related to local reaction within the isolator. The Mach number of the bulk flow returns to supersonic well downstream of the injection region; this occurs in the first few centimeters of the expanding downstream combustor. Mixing and combustion are rapid for this flow-field; predicted combustion efficiency compares well with experimental values.

Wall pressure comparisons between the experiment and the simulation indicate two significant discrepancies; there is (approximately) a 30% underprediction in the upstream interaction distance and (approximately) a 15% overprediction in the peak pressure at the fuel injector and combustor entrance. These differences can be explained qualitatively by further examination of available experimental injected fuel contours which show a distinct movement of the entering vitiated airstream to the sides of the combustor in the experiment, around the injector arrays as a whole. This fact, along with observations regarding the facility nozzle flow-field, leads to the conclusion that the use of jet-to-jet symmetry for such dual-mode problems may not be valid. Requirements for the numerical simulation of this problem include the full modeling of one-half of the combustor duct rather than the symmetry strategy used in this and in previous computational investigations in the literature. This observation may, in fact, extend to low aspect ratio dual-mode scramjet combustors in general since there may be an inherent tendency of the entering airstream to significantly deflect around the entire upstream interaction region in front of multiple-injector arrays. Further study of this effect is warranted; ongoing investigations include the complete half-duct modeling of the same configuration examined in this work.

## ACKNOWLEDGMENTS

This work has been performed under NASA Grant NAG-1189; Charles McClinton, Technology Manager, Hyper-X Program Office, NASA Langley Research Center, is thanked for his support, advice, and guidance at all phases of this work.

## REFERENCES

1. Curran, E. T. and Stall, F. D., "The Utilization of Supersonic Combustion Ramjet Systems at Low Mach Numbers," Aero Propulsion Laboratory, RTD-TDR-63-4097, January 1964.
2. Billig, F. S. and Dugger, G. L., "The Interaction of Shock Waves and Heat Addition in the Design of Supersonic Combustors," *Proceedings of 12<sup>th</sup> Symposium on Combustion*, Combustion Institute, Pittsburgh, PA, 1969, pp. 1125-1134.
3. Billig, F. S., Dugger, G. L., and Waltrup, P. J., "Inlet-Combustor Interface Problems in Scramjet Engines," *Proceedings of the 1<sup>st</sup> International Symposium on Airbreathing Engines*, Marseilles, France, June 1972.
4. Waltrup, P. J. and Billig, F. S., "Prediction of Precombustion Wall Pressure Distribution in Scramjet Engines," *Journal of Spacecraft and Rockets*, Vol. 10, No. 9, 1973, pp. 620-622.
5. Waltrup, P. J. and Billig, F. S., "Structure of Shock Waves in Cylindrical Ducts," *AIAA Journal*, Vol. 11, No. 9, 1973, pp. 1404-1408.
6. Anderson, G. Y., et al., "Experimental Investigation of a Swept-Strut Fuel Injector Concept for Scramjet Application," NASA TN D-8454, August 1977.
7. McClinton, C. R., "Interaction between Step Fuel Injectors on Opposite Walls in a Supersonic Combustor Model," NASA TP-1174, May 1978.
8. Eggers, J. M., Reagon, P. G., and Gooderum, P. B., "Combustion of Hydrogen in a Two-dimensional Duct with Step Fuel Injectors," NASA TP-1159, May 1978.
9. Komuro, T., Kudo, K., Masuya, G., Chinzei, N., Murakami, A., and Tani, K., "Experiment on a Rectangular Cross Section Scramjet Combustor," (in Japanese), National Aerospace Laboratory, NAL TR-1068, Tokyo, Japan, 1990.
10. Murakami, A., Komuro, T., and Kudo, K., "Experiment on a Rectangular Cross Section Scramjet Combustor (II) - Effects of Fuel Injector Geometry," (in Japanese) National Aerospace Laboratory, NAL TR-1220, Tokyo, Japan, 1993.
11. Chinzei, N., et al., "Effects of Injector Geometry on Scramjet Combustor Performance," *AIAA Journal of Propulsion and Power*, Vol. 9, No. 1, January-February 1998, pp. 146-152.
12. Mizobuchi, Y., Matsuo, Y., and Ogawa, S., "Numerical Estimation of Turbulence Temperature Fluctuation Effect on Hydrogen-Oxygen Reaction Process," AIAA Paper 97-0910, January 1997.

13. Matsuo, Y., Mizobuchi, Y., and Ugawa, S., "Parallel Numerical Simulation of Compressible Free Shear Layers in a Scramjet Engine," AIAA Paper 98-0963, January 1998.
14. Heiser, W. H. and Pratt, D. T., Hypersonic Airbreathing Propulsion, AIAA Education Series, American Institute of Aeronautics and Astronautics, Washington, D.C., 1994.
15. Drummond, J. P., Carpenter, M. H., and Riggins, D. W., "Mixing and Mixing Enhancement in Supersonic Reacting Flowfields," High-Speed Flight Propulsion Systems (Chapter 7), Progress in Astronautics and Aeronautics, Vol. 137, AIAA, Washington, D.C., 1991.
16. Wilcox, D. C., "Reassessment of the Scale-Determining Equation for Advanced Turbulence Models," *AIAA Journal*, Vol. 26, No. 11, November 1988, pp. 1299-1310.
17. Menter, F. R., "Improved Two-Equation K- $\omega$  Turbulence Models for Aerodynamic Flows," NASA TM 1103975, October 1992.